



Surface Science

Volume 605, Issues 7-8, Pages L13-L16, 649-858 (April 2011)

- 1 **Editorial Board**
Page IFC

Surface Science Letters

- 2 **Instability of one-dimensional dangling-bond wires on H-passivated C(001), Si(001), and Ge(001) surfaces**
Pages L13-L15
Jun-Ho Lee, Jun-Hyung Cho

Research Highlights

► One-dimensional dangling-bond wires fabricated on C(001), Si(001), and Ge(001) surfaces. ► Peierls instability or spin ordering in one-dimensional wires. ► The C wire has an antiferromagnetic spin ordering. ► The Ge wire has a Peierls-like lattice distortion.

Surface Science

- 3 **Adsorption and desorption of fullerene on graphene/SiC(0001)**
Pages 649-653
Hae-geun Jee, Jin-Hee Han, Han-Na Hwang, Young Dok Kim, Chan-Cuk Hwang

Research Highlights

► Adsorption and desorption of fullerene on single-layer graphene. ► No modification of the band structure of graphene by fullerene. ► Use of fullerene as protection layer of graphene.

- 4 **Structural characterization of Pb nanoislands in SiO₂/Si interface synthesized by ion implantation through MEIS analysis**
Pages 654-658
D.F. Sanchez, F.P. Luce, Z.E. Fabrim, M.A. Sortica, P.F.P. Fichtner, P.L. Grande

Research Highlights

► First structural characterization of buried nanoparticles by MEIS analysis. ► Mean size and number density of the Pb nanoparticles system were determined. ► No accurate information on the nanoparticle geometrical shape for the studied system.

- 5 **STM and XPS investigations of bismuth islands on HOPG**
Pages 659-667
P.J. Kowalczyk, O. Mahapatra, D.N. McCarthy, W. Kozłowski, Z. Klusek, S.A. Brown

Research Highlights

► Metallic character of thin Bi films on graphite was confirmed. ► Layer-pairing was observed. ► Deviations from the bulk atomic arrangement was identified. ► Presence of the second fast growth direction was indicated. ► Atomic resolution images were acquired.

6 **Stability of gold nanostructures on rutile TiO₂(110) surface**

Pages 668-674

T. Pabisiak, A. Kiejna

Research highlights

► Formation of Au nanostructures on the rutile TiO₂(110) with different degree of O reduction. ► Au atoms adsorb strongest at oxygen vacancy sites. ► Potential energy profiles of the adsorbed Au monomers and dimers. ► Stable structures of different shape of two to nine Au atoms were determined. ► Infinitely long Au rows most stable of all investigated structures on the reconstructed TiO₂(110).

7 **Low energy alkali ion scattering investigation of Au nanoclusters grown on silicon oxide surfaces**

Pages 675-680

Snjezana Balaz, Jory A. Yarmoff

Research Highlights

► Au nanocrystals were probed with low energy alkali ion scattering. ► Au nanoclusters were deposited onto various Si oxide surfaces. ► The nanoclusters evolve from single layer to multilayer structures during growth. ► The nanoclusters display quantum effects as their size changes.

8 **A theoretical study of CO adsorption on FeCo(100) and the effect of alloying**

Pages 681-688

Panithita Rochana, Jennifer Wilcox

Research Highlights

► Alloying Fe and Co changes in preferable metal for CO adsorption. ► CO preferentially adsorbs on the Co-site of the FeCo alloys rather than the Fe-site. ► FeCo(100) is more reactive than pure Fe or Co surface due to lower work function. ► d-band center of Co atoms in FeCo alloy moves closer to Fermi level. ► d-band center of Fe atoms in FeCo alloy moves away from the Fermi level.

9 **Quantum nuclear effects on the location of hydrogen above and below the palladium (100) surface**

Pages 689-694

Changjun Zhang, Angelos Michaelides

Research Highlights

► Ab initio path integral molecular dynamics simulations of hydrogen and deuterium adsorbed on/in the Pd(100) surface is reported. ► Significant quantum nuclear effects are found by comparing with conventional ab initio molecular dynamics simulations with classical nuclei. ► Ab initio path integral molecular dynamics simulations of surface and subsurface adsorption are now feasible.

10

Ab initio determination of atomic structure and energy of surface states of bare and hydrogen covered GaN (0001) surface — Existence of the Surface States Stark Effect (SSSE)

Pages 695-713

Paweł Kempisty, Paweł Strąk, Stanisław Krukowski

Research Highlights

► A stable structure of clean GaN(0001) surface possesses (2×1) reconstruction, having every second row of Ga located near plane of N atoms. ► Ga-related dispersionless surface electronic state was obtained, already identified by angle resolved photoelectron spectroscopy. ► For the adsorbate density up to one H atom for each Ga surface atom, the adatoms are located at the on-top positions. ► The H-related quantum surface state is located at valence band maximum (VBM) and deeply in the valence band, about 2 eV below VBM for p- and n-GaN surface, respectively which is related to Surface States Stark Effect (SSSE).

11

Disordered reconstructions of the reduced SnO₂-(110) surface

Pages 714-722

Péter Ágoston, Karsten Albe

Research Highlights

► Extensive search for ground-state structures of the reduced SnO₂-(110) surface. ► Completion of the previously unknown equilibrium surface phase diagram. ► Proposal of a meta-stable surface reconstruction of the SnO₂-(110) surface. ► Assessment of the stability of meta-stable (4 × 1) reconstructions. ► Discussion of expected STM contrast on the basis of Tersoff–Haman calculations.

12

Resonances in the final Rydberg state population of multiply charged ions ArVIII, KrVIII, and XeVIII escaping solid surfaces

Pages 723-732

S.M.D. Galijaš, N.N. Nedeljković, M.D. Majkić

Research Highlights

► We consider the population of Rydberg states of ions escaping solid surfaces. ► We examine the resonances in probability distributions for multiply charged ions. ► The ionic core polarization strongly influences the final distributions. ► The argon anomaly is obtained within the two-state vector model.

- 13 **Effects of adsorbates on the formation of doubly excited He atoms during impact of He^{2+} ions on Fe(110) and Ni(110) surfaces**
 Pages 733-737
 M. Busch, S. Wethekam, H. Winter
- 14 **Properties of rutile TiO_2 surfaces from a Tight-Binding Variable-Charge model. Comparison with *ab initio* calculations**
 Pages 738-745
 A. Hallil, E. Amzallag, S. Landron, R. Tétot

Research Highlights

► Properties of low index rutile TiO_2 surfaces. ► A new Tight-Binding Variable-Charge model for ionic-covalent compounds. ► DFT calculations. ► Surface energies, atomic relaxations and charge transfer.

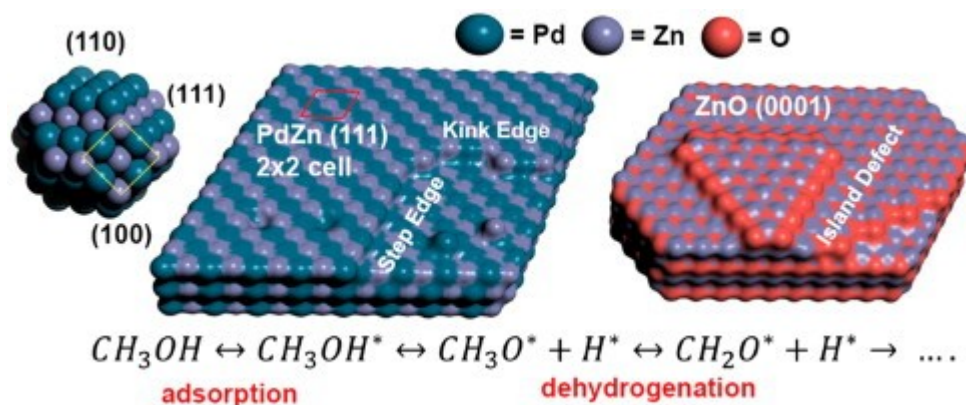
- 15 **Methane adsorption on graphene from *first principles* including dispersion interaction**
 Pages 746-749
 C. Thierfelder, M. Witte, S. Blankenburg, E. Rauls, W.G. Schmidt

Research Highlights

► Benchmarking various dispersion correction schemes (DFT-D, vdW-DF, MP2) at noble gas dimers. ► Microscopic picture of the methane adsorption on graphene. ► Results fit experimental findings.

- 16 **Initial steps in methanol steam reforming on PdZn and ZnO surfaces: Density functional theory studies**
 Pages 750-759
 Gregory K. Smith, Sen Lin, Wenzhen Lai, Abhaya Datye, Daiqian Xie, Hua Guo

Graphical abstract



Research highlights

► CH₃OH and H₂O dissociations on defect-free PdZn surfaces are highly activated.
► Defects on PdZn surfaces lower these barriers. ► CH₃OH and H₂O dissociations on the ZnO(0001) surface have relatively low barriers.

17 **Coverage dependence of glycine adsorption on the Ge(100) – 2 × 1 surface**

Pages 760-769

Jessica S. Kachian, Soon Jung Jung, Sehun Kim, Stacey F. Bent

Research Highlights

► Glycine adsorbs on Ge(100) – 2 × 1 by O–H dissociation. ► Major products are O–H dissociated adducts with some exhibiting N dative bonding. ► Minor product is dual O–H and N–H dissociated adduct. ► Coverage dependent product distribution is observed.

18 **Theoretical study of electric conductance of atomic contact with the Friedel sum rule**

Pages 770-774

Yusuke Kotani, Nobuyuki Shima, Kenji Makoshi

Research Highlights

► We calculate the electric conductances of atomic contacts consisting of Au, Al and Pt based on nonequilibrium Green's function theory and phase shift analysis. ► We analytically introduce the charge neutrality condition through the Friedel sum rule. ► We have analytically shown that the electric conductances are quantized and can increase when the distance between two electrodes increases. ► We conclude that the increment of the electric conductance is interpreted by the Friedel sum rule.

19 **Optical and morphological properties of N-doped TiO₂ thin films**

Pages 775-782

K.G. Grigorov, I.C. Oliveira, H.S. Maciel, M. Massi, M.S. Oliveira Jr., J. Amorim, C.A. Cunha

Research Highlights

► Reducing the band gap width of TiO_x–N_y thin films. ► N-doped TiO₂. ► Reducing the surface energy. ► Hydrophobic properties. ► Selective optical coatings.

20 **Tribological effect of iron oxide residual on the DLC film surface under seawater and saline solutions**

Pages 783-787

R.P.C. Costa, F.R. Marciano, D.A. Lima-Oliveira, E.J. Corat, V.J. Trava-Airoldi

Research Highlights

► The amount of iron mass residual was inversely proportional to the wear rate. ► The

DLC showed dependence behavior with salt concentration of saline solutions. ► The tribofilm on DLC surface increased the disorder of DLC film structure. ► The iron oxide residual decreased the dispersive component of DLC surface energy.

21 **Angle-resolved inverse photoemission of H-etched 6H-SiC (0001)**

Pages 788-792

Nabi Aghdassi, Ralf Ostendorf, Peter Krüger, Helmut Zacharias

Research Highlights

► Angle-resolved inverse photoemission is performed on hydrogen-etched 6H-SiC(0001). ► Etching leads to silicate adlayer on SiC surface. ► No unoccupied Mott-Hubbard surface state observed after flashing samples. ► Saturation of dangling bonds by hydroxyl groups more likely than by hydrogen atoms.

22 **Surface and interface effects on structural transformation of vapor-deposited ethylbenzene films**

Pages 793-798

Ryutaro Souda

Research Highlights

► Transition temperature of a 2D liquid phase of ethylbenzene was determined. ► Roles of the 2D liquid and substrate in finite-size effects on T_g were clarified. ► Quenching of crystallization from thin liquid films was observed.

23 **Effect of subsurface boron on photoluminescence from silicon nanocrystals**

Pages 799-801

Navneethakrishnan Salivati, Nimrod Shuall, Joseph M. McCrate, John G. Ekerdt

Research Highlights

► The effect of boron doping Si nanocrystals on deuterium desorption is reported. ► A hot wire filament is used to dissociated D_2 to D and B_2D_6 to BD_x . ► Deuterium passivates Si dangling bonds and unreconstructs the surface dimer bonds. ► Boron backbonds with the silicon surface atoms and the next layer of silicon. ► The boron enhances nonradiative Auger recombination and quenches photoluminescence.

24 **Decomposition of NH_3 on Ir(110): A first-principle study**

Pages 802-807

Xiang-Zhen Xiao, Yi-Lin Cao, Ying-Ying Cai

Research Highlights

► Finding a tilted off-top adsorption state for NH_3 on Ir(110). ► Presenting a micro picture for NH_3 decomposition. ► Revealing the main factors which influence NH_3 decomposition.

Characterization of Rh, Mo and Rh–Mo particles formed on TiO₂(110) surface: A**TDS, AES and RAIRS study***Pages 808-817*

László Bugyi, Róbert Németh

Research highlights

► HT CO-desorption from TiO₂ + Rh + CO_{sat} corresponds to C+O reaction on the titania support. ► Lack of CO₂ suggests that O atoms arising from CO bind to reduced centers of titania. ► Preformed Mo particles increase the dispersion of rhodium deposit. ► Extended CO dissociation on Mo-Rh particles stems mainly from reaction with Mo. ► The Mo₂C formed is a possible source of enhanced catalytic activity of Mo-Rh clusters.

Surface reactions of AsH₃, H₂Se, and H₂S on the Zn₂TiO₄(010) surface*Pages 818-823*

Shiqiang Hao, Rees B. Rankin, J. Karl Johnson, David S. Sholl

Research Highlights

► Dissociative adsorption of AsH₃, H₂Se and H₂S on Zn₂TiO₄(010) is studied by DFT. ► Fundamental insight into surface chemistry of trace contaminant removal is provided.

Driving forces for the adsorption of cyclopentene on InP(001)*Pages 824-830*

P.P. Favero, A.C. Ferraz, W.G. Schmidt, R. Miotto

Research highlights

► Cyclopentene interaction with InP(001) is investigated by density functional theory. ► A simple approach for evaluating the surface strain is suggested. ► A linear relation between bond (strain) and adsorption energies is established. ► Charge density associated to the HOMO is more disperse for higher bond energies.

STM observations of the first polymerization steps between hexahydroxy-triphenylene and benzene-di-boronic acid molecules*Pages 831-837*

Roland Coratger, Bastien Calmettes, Mathieu Abel, Louis Porte

Research Highlights

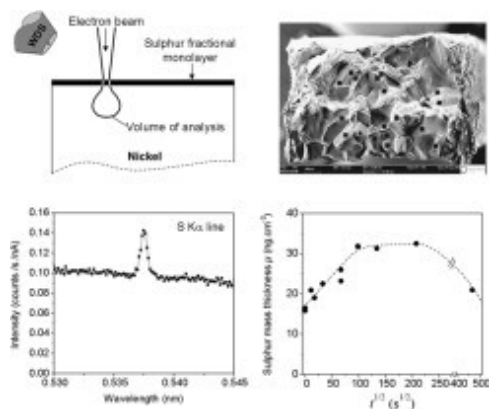
► Observation of the first polymerization steps between benzene-diboronic acid (BDBA) and hexahydroxy-triphenylene (HHTP) molecules. ► STM observations of different HHTP networks on Ag(111). ► STM observations of the oligomer formation. ► Investigations of the first covalent organic structures. ► Vertical manipulation of HHTP using the STM tip.

Research highlights

► Step bunching and step rotation are observed in Si/Si(110)- 16×2 homoepitaxy. ► Step pattern may be tuned by choosing the direction of the electric current. ► Polarity of the applied electrical field has almost no effect the step motion. ► Imperfect matching of the (16×2) reconstruction domains induces step bunching.

Research highlights

► Bi atoms are mobile at low coverage on Rh(111) at RT. ► Bi atoms form incommensurate films on Rh(111) except at 0.5 ML. ► At the coverage of 0.5 ML, Bi atoms form a commensurate structure of $c(2 \times 4)$. ► Bi films transform from twofold structure into sixfold structure above 0.5 ML.

Graphical Abstract**Research Highlights**

► WD X-ray Spectroscopy can be used to quantify grain boundary segregation in a SEM. ► The technique can be used on ex-situ fractured samples. ► The precision and limit of detection is a couple of ng cm^{-2} or percents of a monolayer.